

Collective excitations in the neutron star inner crust

Luc Di Gallo,^{1,*} Micaela Oertel,^{1,†} and Michael Urban^{2,‡}

¹*LUTH, Observatoire de Paris, CNRS, Université Paris Diderot, 5 place Jules Janssen, 92195 Meudon, France*

²*Institut de Physique Nucléaire, CNRS/IN2P3 and Université Paris Sud 11, 91406 Orsay, France*

We study the spectrum of collective excitations in the inhomogeneous phases in the neutron star inner crust within a superfluid hydrodynamics approach. Our aim is to describe the whole range of wavelengths, from the long-wavelength limit which can be described by macroscopic approaches and which is crucial for the low-energy part of the spectrum, to wavelengths of the order of the dimensions of the Wigner-Seitz cells, corresponding to the modes usually described in microscopic calculations. As an application, we will discuss the contribution of these collective modes to the specific heat of the “lasagna” phase in comparison with other known contributions.

PACS numbers: 26.60.Gj

I. INTRODUCTION

Neutron stars are fascinating objects, containing matter under extreme conditions of temperature, density and magnetic field. In order to study these celestial bodies, theoretical modeling has to be confronted with observations. A prominent observable is the thermal evolution of isolated neutron stars. Properties of the crust thereby influence the cooling process mainly during the first 50-100 years, when the crust stays hotter than the core which cools down very efficiently via neutrino emission (see e.g. [1]). Heat transport in the crust is the key ingredient to explain the afterburst relaxation in X-ray transients, too [2, 3]. Concerning the models for the thermal relaxation of the crust, the most important microscopic ingredients are thermal conductivity and heat capacity, and to less extent neutrino emissivities. Here, as a first application, we will concentrate on the heat capacity. More details about the evaluation of the heat capacity and a discussion of the usually considered contributions can be found in [4]. In what follows, we will concentrate on the particularly interesting case of the neutron star inner crust.

The core of neutron stars is composed most probably of homogeneous neutron rich matter, whereas the crust contains different inhomogeneous structures. The inner crust is thereby characterized by the transition from a lattice of atomic nuclei in the outer crust to homogeneous matter in the core. Ravenhall et al. [5] and Hashimoto et al. [6] predicted that this transition passes via more and more deformed nuclei. Starting from an almost spherical shape, they could form rods or slabs immersed in a neutron gas at the different densities. These “spaghetti” and “lasagna” phases are commonly called the nuclear “pasta”. At higher densities, even closer to the core, other phases such as neutron-gas bubbles inside the dense matter (“swiss cheese” phase) etc. are expected. The

formation of the different structures strongly depends on the relative strength of the nuclear surface energy, Coulomb energy and bulk energy, such that it depends on the nuclear interaction. This prediction has been confirmed within different models for the nuclear interaction, see, e.g., [7–10]. These evaluations have been performed at zero temperature. It is clear that at some critical temperature the pasta structures will disappear due to thermal excitations. However, this melting temperature is of the order of several MeV (see e.g. [11, 12]).

Another point is that in neutron stars older than several minutes, matter becomes superfluid. A first evidence for superfluidity in neutron stars has been discussed already in 1969 [13], shortly after the discovery of the first pulsars, in connection with the observation of “glitches”. Since then much effort has been devoted to the question of superfluidity and superconductivity in neutron star matter, for the inner crust as well as for the homogeneous core, see for example [8]. There is no consensus on the exact value of the energy gaps Δ in the inner crust [14, 15], but the common agreement is that they are of the order of 1 MeV [16]. A pairing gap much larger than the temperature strongly suppresses the contribution of individual neutrons to the specific heat which is thus very much dependent on the pairing strength [4, 17]. For moderate and strong pairing, the main contributions to the heat capacity considered so far in the crust are thus electrons and lattice vibrations as well as collective excitations of nuclei. However, the superfluid character of neutron star matter induces collective excitations of the neutron gas, not considered before, which can give an important contribution to the heat capacity in certain regions, see [18–20].

The aim of the present paper is to study these collective excitations in the inner crust employing a superfluid hydrodynamics approach. Naturally, there is a vast literature on hydrodynamics for neutron stars in different contexts, including the effects of superfluidity [21–27]. Most of these models are dedicated to the study of macroscopic neutron star properties, whereas our main aim is to study the excitation spectrum of the crust on much smaller length scales. In spirit this is similar to Refs. [19, 20, 28], where hydrodynamic equations are de-

*Electronic address: luc.digallo@obspm.fr

†Electronic address: micaela.oertel@obspm.fr

‡Electronic address: urban@ipno.in2p3.fr

veloped to study the superfluid Goldstone boson and (lattice) phonons in the long wavelength limit. However, we are interested in shorter wavelengths at which effects of the inhomogeneous structure will manifest themselves, too. In this sense, our approach is situated in between the long wavelength limit and the completely microscopic calculations (see e.g. [17, 29, 30]) employing the Wigner-Seitz approximation [31]. In the latter case, the wavelengths are limited to the size of the Wigner-Seitz cell, because of the imposed boundary conditions which do not include the coupling between neighboring cells.

The paper is organized as follows. In Sec. II, we describe the superfluid hydrodynamics approach. We summarize the hydrodynamic equations, discuss the boundary conditions and the microscopic input. In Sec. III, we show our first results. For simplicity, we restrict ourselves to one-dimensional inhomogeneities (lasagna phase) in this exploratory study. We discuss the spectrum of the collective modes and their contributions to the specific heat. A summary and perspectives of our work are exposed in Section IV.

Throughout the article, c , \hbar , and k_B denote the speed of light, the reduced Planck constant, and the Boltzmann constant, respectively.

II. MODEL

A. Superfluid hydrodynamics approach

In this paper, we are interested in temperatures below $\sim 10^9$ K, which is very small compared to the gap energy Δ . Therefore we can use the zero temperature approximation, thus assuming that there are no normal fluids but only superfluids. In this limit, the dynamics of a superfluid system with slow temporal and spatial variations is completely determined by the dynamics of the phase of the order parameter: If the superfluid order parameter is written as $\Delta(\mathbf{r}) = |\Delta(\mathbf{r})|e^{i\phi(\mathbf{r})}$, the superfluid velocity is given by $\mathbf{v}_s = (\hbar/2m)\nabla\phi$ [32], m being the nucleon mass. Actually, as pointed out in Ref. [33], the phase of the order parameter determines the momentum per particle $\mathbf{p} = m\mathbf{v}_s$ and not the fluid velocity \mathbf{v} . This distinction is important in the context of “entrainment” in a system containing protons and neutrons, see below.

An important length scale is the superfluid coherence length, $\xi_0 = \hbar v_F/\pi\Delta$ [34], where v_F denotes the Fermi velocity. It varies from several fm up to tens of fm for typical values of the densities, neutron fractions, and gaps in the inner crust. As can be shown by deriving the equations of superfluid hydrodynamics from the microscopic time-dependent Bogoliubov-de Gennes (or Hartree-Fock-Bogoliubov) equations [35, 36], the hydrodynamic approach is valid if the length scale of spatial variations is larger than ξ_0 , and frequencies are small compared with Δ/\hbar . As will be discussed later on, for the concrete examples we consider, we are at the limits of validity of the approach. However, considering the tremendous dif-

ficulties to perform completely microscopic calculations beyond the Wigner-Seitz approximation, we leave such investigations for the future and consider our approach sufficient for the moment.

In addition, we will neglect the Coulomb interaction of the protons. This represents an enormous simplification, but at the same time it implies that we cannot correctly reproduce the phonons of the Coulomb lattice. In homogeneous matter, too, the Coulomb interaction plays an important role for the collective modes, in particular the coupling of the proton plasmon mode with the electrons as discussed in [37, 38], but it is beyond the scope of the present paper. Our main focus lies therefore on the dynamics of the neutron gas, which is however coupled to the proton dynamics due to the nuclear interaction.

In principle, the equations of superfluid hydrodynamics can be derived from the underlying microscopic theory, as it was done for the case of ultracold trapped fermionic atoms in [35, 36]. Here, we follow the simpler way to derive them from local conservation laws. Since the fluid velocities and the densities are low enough, we will use a non-relativistic formulation.

The first conservation law is neutron and proton number conservation [51]. This results in two continuity equations, one for neutrons ($a = n$) and one for protons ($a = p$),

$$\partial_t n_a + \nabla \cdot (n_a \mathbf{v}_a) = 0, \quad (1)$$

where n_a denotes the particle number density of species a .

The second conservation law, the conservation of momentum, results in the Euler equations, which can be written as

$$n_a (\partial_t \mathbf{p}_a + \nabla \tilde{\mu}_a) = 0, \quad (2)$$

where $\tilde{\mu}_a$ is the rest-frame chemical potential defined as the conjugate momentum with respect to the particle density n_a in a variational approach [39]. The explicit expression is

$$\tilde{\mu}_a = \mu_a + \mathbf{v}_a \cdot \mathbf{p}_a - \frac{1}{2} m_a v_a^2, \quad (3)$$

where μ_a is the local chemical potential of species a . Due to the interaction between neutrons and protons, μ_a depends on the densities of both species.

In pure neutron matter, the momentum \mathbf{p}_n is simply given by $\mathbf{p}_n = m_n \mathbf{v}_n$. However, in a system containing neutrons and protons, the two species drag each other due to their interaction. In the theory of superfluids, this effect is known as entrainment [40]. As a consequence, fluid momenta are misaligned with particle velocities. The relationship between the velocity and the momentum can be expressed via the entrainment matrix (also called Andreev-Bashkin or mass-density matrix) [33]:

$$m_a n_a \mathbf{v}_a = \sum_{b=n,p} \rho_{ab} \frac{\mathbf{p}_b}{m_b}. \quad (4)$$

In practice, at densities which are relevant in the inner crust, the non-diagonal elements of ρ are small [33], i.e.,

$$\rho_{ab} \approx m_a n_a \delta_{ab}. \quad (5)$$

B. Microscopic input

As microscopic input, we need the equation of state, i.e., the relation between the densities n_a and the chemical potentials μ_a , and the entrainment matrix ρ . In our concrete numerical examples, we will use the results of the work by Avancini et al. [10] for the equilibrium configurations. They evaluate the structure of the pasta phases for charge neutral matter in β equilibrium using a density dependent relativistic mean-field model, the DDH δ model (originally called DDH $\rho\delta$) [10, 41, 42], for the nuclear interaction. In order to be consistent, we shall calculate the chemical potentials μ_a and the entrainment matrix ρ with the same interaction. For the entrainment matrix, we closely follow Gusakov et al. [43], who generalized the determination of the entrainment matrix for neutron-proton mixtures based on Landau-Fermi liquid theory [44] to relativistic models. The only modification of the expressions in Ref. [43] we have to perform is due to the presence of the isovector-scalar δ meson in the DDH δ model, which modifies the Dirac effective nucleon mass. In particular, the latter is no longer the same for neutrons and protons. Since our hydrodynamic equations are formulated non-relativistically, we consider only the non-relativistic limit of the entrainment matrix ($\rho_{ab} = m_a m_b c^2 Y_{ab}$ in the notation of [43]).

C. Linearization around stationary equilibrium

In order to proceed we will linearize Eqs. (1) and (2) around stationary equilibrium. Let us write the different quantities as a sum of their equilibrium value and a perturbation, $X = X_{\text{eq}} + \delta X$ (in the case of the velocities and momenta we will write the perturbation simply as \mathbf{v}_a and \mathbf{p}_a , respectively, since the equilibrium values of these quantities are zero). The equations can be simplified a lot, since all temporal and spatial derivatives of equilibrium quantities vanish (except at phase boundaries, which will be treated in the next subsection). Eqs. (1) and (4) then reduce to

$$\partial_t \delta n_a = - \sum_{b=n,p} \frac{\rho_{ab,\text{eq}}}{m_a m_b} \nabla \cdot \mathbf{p}_b, \quad (6)$$

and Eqs. (2) and (3) become

$$\partial_t \mathbf{p}_a = - \nabla \delta \mu_a. \quad (7)$$

We will now express the variation of the densities in Eq. (6) in terms of the variation of the chemical potentials,

$$\delta n_a = \sum_{b=n,p} J_{ab} \delta \mu_b, \quad (8)$$

where

$$J_{ab} = \left(\frac{\partial n_a}{\partial \mu_b} \right)_{\text{eq}}. \quad (9)$$

Inserting the resulting equation into the divergence of Eq. (7) one obtains the following system of two coupled wave equations for $\delta \mu_n$ and $\delta \mu_p$:

$$\sum_{b=n,p} (KJ)_{ab} \partial_t^2 \delta \mu_b = \nabla^2 \delta \mu_a, \quad (10)$$

where K is the inverse of the matrix

$$(K^{-1})_{ab} = \frac{\rho_{ab,\text{eq}}}{m_a m_b}. \quad (11)$$

The coupling arises from the non-diagonal elements of the matrices J and K due to the neutron-proton interaction. Let us now make the ansatz that the perturbations have the form of a plane wave, $\delta \mu_a(\mathbf{r}, t) = U_a e^{-i\omega t + i\mathbf{k} \cdot \mathbf{r}}$. Eq. (10) can then be written as a 2×2 eigenvalue problem

$$\sum_{b=n,p} (KJ)_{ab} U_b = \frac{1}{u^2} U_a, \quad (12)$$

with $u = \omega/k$ denoting the sound velocity. The two eigenvalues give two sound velocities which we will label u^\pm . Note that the corresponding eigenvectors, U_a^\pm , do not describe pure proton or neutron waves, but combinations of both. We denote by $+$ and $-$ the modes where neutrons and protons oscillate in phase and out of phase, respectively.

In the special case of pure neutron matter, there is only one mode, which can be obtained from the above equations by setting $n_p = 0$. Its sound velocity is given by

$$u^2 = \left(\frac{n_n}{m_n} \frac{\partial \mu_n}{\partial n_n} \right)_{\text{eq}}. \quad (13)$$

D. Boundary conditions

In our model, we consider the inhomogeneous phases in the inner crust as mixed phases where a neutron gas (phase 1) coexists with a dense phase (phase 2) containing neutrons and protons. However, in order not to have to write everything separately for phase 1 and phase 2, we will write all equations, unless otherwise stated, for the general case that neutrons and protons are present in both phases. The equations relevant for phase 1 can easily be obtained by considering the special case $n_{p1} = 0$. The fact that both phases coexist implies that in equilibrium the chemical potentials and pressures are equal in both phases: $\mu_{a1} = \mu_{a2}$ and $P_1 = P_2$. The description of the interface between the two phases requires a microscopic formalism and is beyond the scope of this work.

In our model, we assume that the hydrodynamic equations are valid in both the gas and the dense phase, but

since they do not say anything about the behavior at the interface, they have to be supplemented by appropriate boundary conditions. The first boundary condition arises from the obvious requirement that contact has to be maintained at all times at the interface [45]. Therefore, the displacement normal to the interface has to be continuous and equal for all components ($a = n, p$) at all times. Hence, the velocities normal to the interface must satisfy:

$$v_{\perp n1}(\mathbf{r}) = v_{\perp p1}(\mathbf{r}) = v_{\perp n2}(\mathbf{r}) = v_{\perp p2}(\mathbf{r}). \quad (14)$$

The second boundary condition arises from the requirement that the pressure P on both sides of the interface must be equal [46]:

$$P_1(\mathbf{r}) = P_2(\mathbf{r}). \quad (15)$$

If we linearize this condition, it can be written as

$$\sum_{a=n,p} n_{a1}(\mathbf{r})\delta\mu_{a1}(\mathbf{r}) = \sum_{a=n,p} n_{a2}(\mathbf{r})\delta\mu_{a2}(\mathbf{r}), \quad (16)$$

where the index eq after n_{a1} and n_{a2} has been dropped for brevity.

Before applying our model to the neutron-star inner crust, let us see whether these boundary conditions give reasonable results for collective modes in isolated nuclei. For simplicity, we will consider a nucleus with equal numbers of neutrons and protons ($N = Z = A/2$). Within the hydrodynamic model, the nucleus is a homogeneous sphere with a sharp surface at $r = R$. The proton and neutron densities inside the nucleus are $n_n = n_p = n_0/2$, where $n_0 = 0.153 \text{ fm}^{-3}$ is the saturation density within the DDH δ model. As a first example, we consider the isoscalar monopole mode, where neutrons and protons oscillate together in radial direction. The solution of the wave equation inside the nucleus is $\delta\mu_n = \delta\mu_p \propto j_0(\omega r/u^+)$, where j_l is a spherical Bessel function and $u^+ = 0.169 c$ is the sound velocity for the in-phase oscillation of neutrons and protons. Since protons and neutrons move together, the first boundary condition (14) is automatically satisfied, while the second one, Eq. (16), requires $\delta\mu(r = R) = 0$. Consequently, the energy of the monopole mode is $\hbar\omega = \pi\hbar u^+/R \approx 90 \text{ MeV}/A^{1/3}$.

Another interesting simple case is the isovector giant-dipole resonance (GDR), where neutrons and protons oscillate against each other in z direction. In this case, our approach is identical to the Steinwedel-Jensen model of the GDR [47]. Again, the solution of the wave equation is straight-forward and gives $\delta\mu_n = -\delta\mu_p \propto j_1(\omega r/u^-)\cos\theta$, where θ is the angle between \mathbf{r} and the z axis, and $u^- = 0.233 c$ is the sound velocity for the out-of-phase oscillation of neutrons and protons. In this case, the second condition (16) is automatically fulfilled, but now the first one, Eq. (14), becomes relevant. Using the Euler equation (7), one can show that the radial component of the velocity field is proportional to $v_{rn} = -v_{rp} \propto \partial\delta\mu/\partial r \propto j_1'(\omega r/u^-)\cos\theta$, so that Eq. (14) gives $\hbar\omega = 2.08\hbar u^-/R \approx 82 \text{ MeV}/A^{1/3}$.

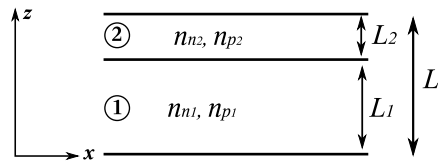


FIG. 1: Diagram representing the slab structure.

These results for the isoscalar monopole and the isovector GDR are quite reasonable, at least for heavy nuclei, although their energies are much higher than the pairing gap Δ , such that superfluid hydrodynamics should strictly speaking not be applicable. The reason is that for these particular resonances (contrary to, e.g., the quadrupole mode [48]) the Fermi-surface distortion does not play any role, so that hydrodynamics works even in the normal phase without pairing. We conclude that, at least in some cases, the limits of validity of the hydrodynamic approach may be interpreted very generously.

E. Collective modes in a periodic slab structure

Because of their electric charge, the droplets (or rods, or slabs) of the dense phase arrange in a regular periodic lattice in order to minimize the Coulomb energy. Charge neutrality on a macroscopic scale is guaranteed by the presence of an almost uniform, strongly degenerate electron gas. The size and form of the structures is determined by the interplay of Coulomb energy (favoring small structures) and surface energy (favoring large structures). Since both the Coulomb and the surface energy are neglected in our approach, the determination of the size and form of the structures in equilibrium is beyond the scope of our work. Instead, we will consider the equilibrium geometry as input and calculate the collective oscillations in this geometry. For simplicity, we will restrict ourselves to the simplest geometry which is a structure of periodically alternating slabs with different proton and neutron densities as illustrated in Fig. 1 (lasagna phase). To be specific, we will consider the slabs to be perpendicular to the z axis.

Our aim is to describe the collective modes of this structure. The equilibrium properties of the structure itself, i.e., the densities n_{n1} , n_{p1} , n_{n2} and n_{p2} , and the slab thicknesses L_1 and L_2 , are input parameters which we take from Ref. [10]. The excitations are then obtained by solving in each slab the wave equation (10) together with the boundary conditions (14) and (16) at the interfaces between neighboring slabs.

At each phase boundary, the waves will be partially (or totally) reflected. It is therefore not sufficient to make a plane-wave ansatz in each slab, but one has to consider the reflected wave, too. Thus, we can make the following

ansatz in each slab:

$$\delta\mu_a(\mathbf{r}, t) = \sum_{\sigma=\pm} e^{-i\omega t + i\mathbf{k}_{\parallel} \cdot \mathbf{r}_{\parallel}} \left(\alpha^{\sigma} e^{ik_z^{\sigma} z} + \beta^{\sigma} e^{-ik_z^{\sigma} z} \right) U_a^{\sigma}, \quad (17)$$

where U_a^{\pm} denote the normalized eigenvectors of Eq. (12), $\mathbf{k}_{\parallel} = (k_x, k_y, 0)$ and $\mathbf{r}_{\parallel} = (x, y, 0)$ are the components of \mathbf{k} and \mathbf{r} parallel to the slab, and the k_z^{\pm} have to satisfy

$$k_z^{\pm 2} = \frac{\omega^2}{u^{\pm 2}} - k_{\parallel}^2. \quad (18)$$

Note that k_z^{\pm} can be real or imaginary. The velocities \mathbf{v}_a can be expressed in terms of the coefficients α^{\pm} and β^{\pm} , too. By using the Euler equation (7), one finds that for a plane wave with wave vector \mathbf{k} the velocity field is given by

$$\mathbf{v}_a = \frac{\mathbf{k}}{n_a \omega} \sum_b (K^{-1})_{ab} \delta\mu_b. \quad (19)$$

If we define

$$V_a^{\pm} = \frac{1}{n_a} \sum_b (K^{-1})_{ab} U_b^{\pm}, \quad (20)$$

the superposition of plane waves according to Eq. (17) gives

$$v_{za} = \sum_{\sigma=\pm} \frac{k_z^{\sigma}}{\omega} e^{-i\omega t + i\mathbf{k}_{\parallel} \cdot \mathbf{r}_{\parallel}} \left(\alpha^{\sigma} e^{ik_z^{\sigma} z} - \beta^{\sigma} e^{-ik_z^{\sigma} z} \right) V_a^{\sigma} \quad (21)$$

and a similar relation for \mathbf{v}_{\parallel} .

The next step is to determine the coefficients α^{\pm} and β^{\pm} by matching the solutions in neighboring slabs according to the boundary conditions. If we use indices 1, 2, 3 in order to indicate the quantities in three consecutive slabs, we have perturbations $\delta\mu_{a1}$ valid for $0 < z < L_1$, $\delta\mu_{a2}$ for $L_1 < z < L \equiv L_1 + L_2$, and $\delta\mu_{a3}$ for $L < z < L + L_1$ with four unknown amplitudes, α^{\pm} and β^{\pm} , in each slab. Note that due to the periodicity the equilibrium properties of slab 3 are equal to those of slab 1, but the coefficients α^{\pm} and β^{\pm} are in general different in slabs 1 and 3.

Written explicitly, the boundary conditions are

$$\begin{aligned} v_{zp2}(z = L_1) &= v_{zn2}(z = L_1), \\ v_{zn1}(z = L_1) &= v_{zn2}(z = L_1), \\ v_{zp1}(z = L_1) &= v_{zn2}(z = L_1), \\ \sum_{a=n,p} n_{a1} \delta\mu_{a1}(z = L_1) &= \sum_{a=n,p} n_{a2} \delta\mu_{a2}(z = L_1), \end{aligned} \quad (22)$$

and four analogous equations relating quantities of slabs 2 and 3 at $z = L$.

It is evident that, in order to satisfy the conditions for all \mathbf{r}_{\parallel} , the components \mathbf{k}_{\parallel} must be equal in all three slabs, i.e.,

$$\mathbf{k}_{\parallel 1} = \mathbf{k}_{\parallel 2} = \mathbf{k}_{\parallel 3} \equiv \mathbf{q}_{\parallel}. \quad (23)$$

So far, the boundary conditions give us eight equations for the twelve unknown coefficients $\alpha_1^{\pm}, \dots, \beta_3^{\pm}$. In order to close the system of equations, we have to take into account translational invariance of the system. This can be expressed via the Floquet-Bloch theorem [49]:

$$\delta\mu_a(\mathbf{r} + \mathbf{R}, t) = e^{i\mathbf{q} \cdot \mathbf{R}} \delta\mu_a(\mathbf{r}, t), \quad (24)$$

where \mathbf{q} is the Bloch momentum and $\mathbf{R} = (R_x, R_y, R_z)$ is a vector such that the system is invariant under a shift $\mathbf{r} \rightarrow \mathbf{r} + \mathbf{R}$. In our case, \mathbf{R}_{\parallel} can be arbitrary, but R_z has to be a multiple of the periodicity L , see Fig. 1. With respect to \mathbf{R}_{\parallel} , the condition (24) is automatically satisfied due to Eq. (23). But in the case $\mathbf{R} = (0, 0, L)$, Eq. (24) implies in particular

$$\delta\mu_{a3}(x, y, z = L, t) = e^{iq_z L} \delta\mu_{a1}(x, y, z = 0, t) \quad (25)$$

and an analogous relation for the velocity. Inserting this into the boundary conditions at the interface between slabs 2 and 3 at $z = L$, we obtain

$$\begin{aligned} v_{zp2}(z = L) &= v_{zn2}(z = L), \\ e^{iq_z L} v_{zn1}(z = 0) &= v_{zn2}(z = L), \\ e^{iq_z L} v_{zp1}(z = 0) &= v_{zn2}(z = L), \\ e^{iq_z L} \sum_{a=n,p} n_{a1} \delta\mu_{a1}(z = 0) &= \sum_{a=n,p} n_{a2} \delta\mu_{a2}(z = L), \end{aligned} \quad (26)$$

i.e., we have now a system of eight equations, Eqs. (22) and (26), for eight coefficients $\alpha_1^{\pm}, \dots, \beta_2^{\pm}$.

This system of equations has a non-trivial solution if the determinant of the corresponding 8×8 matrix vanishes. For a given choice of q_{\parallel} and q_z (q_z may be limited to the first Brillouin zone, i.e., $-\pi/L < q_z < \pi/L$), this gives us an equation for ω with an infinite number of discrete solutions.

Note that, as mentioned before, in the case we will actually consider, the proton density vanishes in slab 1 (and 3). In this case, the proton velocity is not defined in that slab and we have only two coefficients α_1 and β_1 instead of four coefficients α_1^{\pm} and β_1^{\pm} , since in pure neutron matter there is only one eigenmode instead of two. The number of equations is also reduced by two, since the third equation of Eqs. (22) and the third equation of Eqs. (26) can be removed. We are therefore left with a 6×6 instead of 8×8 problem. In this case, it is interesting to notice that there are two different types of modes: Modes propagating through all slabs, whose energies depend on q_z , and modes of the dense slabs (slab 2) only, whose energies are independent of q_z . The latter are modes where protons and neutrons oscillate against each other such that at the boundaries ($z = L_1$ and $z = L$) v_{zn} , v_{zp} , and δP vanish simultaneously (analogous to the isovector GDR in an isolated nucleus, discussed at the end of the previous subsection).

When looking for the solutions for ω , one has to be careful to retain only physical solutions. It is easy to see

TABLE I: Properties of the lasagna phase within the model by Avancini et al. [10] studied in our example. The average densities of the total system are given by $n_n = (L_1/L)n_{n1} + (L_2/L)n_{n2}$ etc. Baryon density and proton fraction are defined as $n_B = n_n + n_p$ and $Y_p = n_p/n_n$, respectively.

		slab 1	slab 2	total
L	(fm)	9.40	7.38	16.78
n_n	(fm ⁻³)	0.0701	0.0885	0.0782
n_p	(fm ⁻³)	0	0.0041	0.0018
$n_B = n_n + n_p$	(fm ⁻³)	0.0701	0.0926	0.0800
$Y_p = n_p/n_B$		0	0.0447	0.0227
u or u^+	(c)	0.0641	0.0354	
u^-	(c)		0.1369	

that if one of the three wave numbers k_{z1} , k_{z2}^+ , or k_{z2}^- vanishes, i.e., if ω/q_{\parallel} equals one of the three sound velocities u_1 , u_2^+ , or u_2^- , the system of equations is solved by choosing the corresponding coefficients as $\alpha = -\beta$ and setting all the other coefficients equal to zero. However, this solution implies $\delta\mu = 0$ and therefore does not correspond to a physical excitation.

III. RESULTS FOR THE LASAGNA PHASE

A. Excitation spectrum

Let us now investigate the resulting excitation spectrum for a specific example. As mentioned before, the values for the equilibrium quantities will be taken from the work by Avancini et al. [10], who have studied the structure of pasta phases in a relativistic mean field model. Our geometry corresponds to the lasagna phase, appearing close to the transition to uniform matter in the core, which has been found in Ref. [10] in the case of zero temperature and β -equilibrium for baryon number densities $0.077 \text{ fm}^{-3} \lesssim n_B \lesssim 0.084 \text{ fm}^{-3}$, in good agreement with the results by Oyamatsu [7]. For our example we have chosen an intermediate density, $n_B = 0.08 \text{ fm}^{-3}$. The corresponding properties of the two phases 1 and 2 are listed in Table I.

With the actual numbers for the densities and the dimensions of the structure, the coherence length for a gap of 1 MeV is of the same order of magnitude as the size of the layers, i.e. the scale for spatial variations. That means that our superfluid hydrodynamics approach touches its limit of validity for this example. Strictly speaking, we should also limit ourselves to energies which are small compared to Δ . However, there are many cases where the hydrodynamic approach works reasonably well although its initial assumptions are not fulfilled. Examples are the dipole and monopole resonances in ordinary nuclei mentioned in the preceding section, or the ‘‘super-giant resonances’’ in spherical Wigner-Seitz cells used to model the neutron-star inner crust, whose

excitation energies agree well with an estimate obtained from the sound velocity of the hydrodynamic Bogoliubov-Anderson mode [30].

After this remark of caution, let us discuss the solutions for the energies ω shown in Fig. 2 as functions of $q \equiv |\mathbf{q}|$ for three different angles θ between \mathbf{q} and the z axis (i.e., $q_z = q \cos \theta$ and $q_{\parallel} = q \sin \theta$). The left panel shows the dispersion relation for waves propagating in z -direction, i.e. perpendicular to the interfaces between the different slabs. One observes an acoustic branch with an approximately linear dispersion law

$$\omega = u_s q \quad (27)$$

at low energies, and several optical branches with a finite energy for $q = 0$, analogously to phonons branches in a crystal.

Note that within the Wigner-Seitz approximation, which is usually employed in microscopic calculations [17, 29, 30], we would only obtain a discrete spectrum corresponding to our spectrum in the case $q = 0$. The reason is that in this approximation the coupling between cells is neglected, and thus each cell has the same excitation spectrum. The degeneracy of the modes in each cell is lifted by the coupling between cells, which gives rise to a momentum dependent spectrum as obtained in our approach.

The slope of the acoustic branch, i.e., the speed of sound, coincides (see dashed line in Fig. 2) with the usual thermodynamic expression for the sound velocity

$$u_s^2 = \frac{1}{m} \frac{\partial P}{\partial n_B} \Big|_{Y_p}, \quad (28)$$

where n_B is the average baryon density of the inhomogeneous phase. To evaluate this derivative, we squeeze or expand our unit cell of length L by a small amount $\delta L = \delta L_1 + \delta L_2$. From the requirement $\delta P_1 = \delta P_2 = \delta P$ we can determine δL_1 and δL_2 and thus δP . The final result can be written in a compact form as

$$\frac{L}{n_B u_s^2} = \frac{L_1}{n_{B1} u_{s1}^2} + \frac{L_2}{n_{B2} u_{s2}^2}, \quad (29)$$

where we have defined for each phase $i = 1, 2$

$$u_{si}^2 = \frac{1}{m} \frac{\partial P_i}{\partial n_{Bi}} \Big|_{Y_{pi}}. \quad (30)$$

Note that u_{s1} is identical to the sound velocity u_1 [cf. Eq. (13)], whereas u_{s2} is different from the two sound velocities u_2^{\pm} .

This linear branch corresponds roughly to the long wavelength limit discussed in Ref. [19, 20] although, of course, the numerical value of the sound speed is not the same because we neglect elastic effects of the proton lattice due to Coulomb interaction. At higher wave vectors q , there are deviations from the linear behavior related to the inhomogeneous structure. At these energies the long wavelength limit is no longer valid.

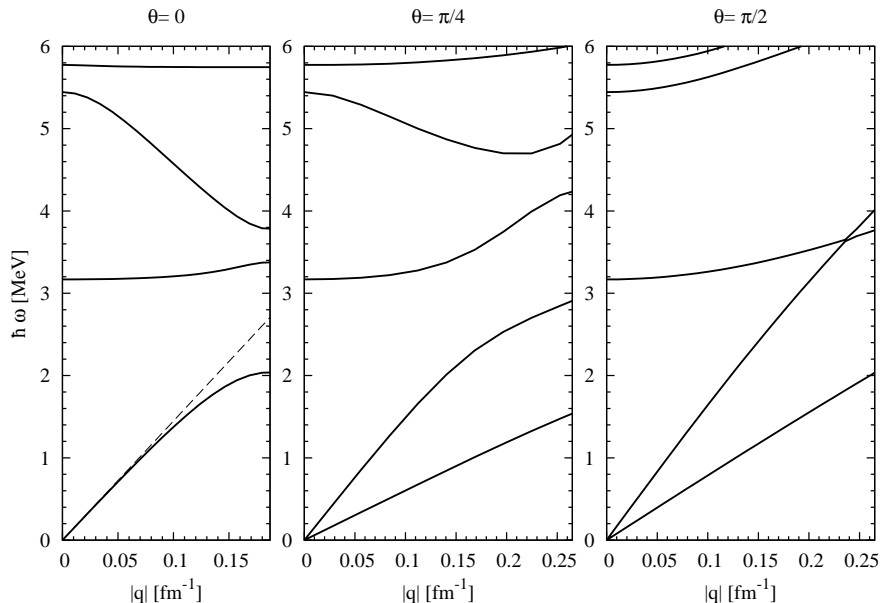


FIG. 2: Dispersion relation of the modes propagating along the z -axis ($\theta = 0$, left), at an angle of 45° ($\theta = \pi/4$, center), and in the plane parallel to the slabs ($\theta = \pi/2$, right). The dashed line in the left panel corresponds to the approximation Eq. (27).

The central and right panels of Fig. 2 show the excitation spectrum for different values of the angle, $\theta = \pi/4$ and $\pi/2$, respectively. One observes that the slope of the acoustic branch discussed before changes: in the present example, u_s increases from $0.072c$ in the case $\theta = 0$ to $0.085c$ in the case $\theta = \pi/2$. The reason is that the wave, which is perfectly longitudinal ($\mathbf{v} \parallel \mathbf{q}$) in the case $\theta = 0$, becomes more complicated in the case $\theta \neq 0$ and the nucleons oscillate now in both longitudinal and transverse directions. But the most important consequence of non-zero angle θ is the appearance of a second acoustic branch, whose slope is strongly angle dependent. In fact, if one writes the energy of this new branch as

$$\omega = u'_s q_{\parallel} = u'_s q \sin \theta, \quad (31)$$

the “two-dimensional sound velocity” u'_s defined by this equation depends only weakly on q_z and q_{\parallel} : in the present example, u'_s varies between $0.04c$ for $q_z \ll q_{\parallel}$ and $0.046c$ for $q_{\parallel} \ll q_z$. A detailed analysis of the solutions for the coefficients α and β corresponding to this branch shows that in this mode, the protons and neutrons oscillate practically only in the direction parallel to the slabs (i.e., $v_z \approx 0$), and the motion takes essentially place in the dense phase.

B. Application to specific heat

We are interested here in the contribution of the above discussed excitation modes to the specific heat. The specific heat, the heat capacity for constant volume per unit

volume, is defined as

$$c_v(T) = \left. \frac{\partial \epsilon}{\partial T} \right|_n, \quad (32)$$

where ϵ denotes the energy density. The contribution of the collective modes can be calculated as follows:

$$\epsilon(T) = \int_{-\pi/L}^{\pi/L} \frac{dq_z}{2\pi} \int \frac{d^2 q_{\parallel}}{(2\pi)^2} \sum_i \hbar \omega_i(\mathbf{q}) \frac{1}{e^{\hbar \omega_i(\mathbf{q})/k_B T} - 1}. \quad (33)$$

Note that we suppose here that the energies $\omega_i(\mathbf{q})$ depend only very weakly on temperature such that it is justified to neglect their temperature dependence. This should be a good approximation as long as the temperature stays well below the value of the energy gap and we therefore have no significant contribution from a normal fluid. Another type of temperature dependence could arise from a change in the structure of the pasta phases. At the temperatures considered here, however, we do not expect a significant effect either since the structure starts to be modified considerably only at higher temperatures [11, 12].

In Fig. 3 we show the different contributions to the specific heat in the density range where the model by Avancini et al. [10] predicts the lasagna phase, for a typical temperature of 10^9 K. Besides the contribution of the collective modes (solid line), we display for comparison the contribution of the electrons (dashed line), which are considered as a practically uniform ultra-relativistic ($\mu_e \gg m_e c^2$) ideal Fermi gas with number density $n_e = n_p$. At low temperature, the electron gas is strongly de-

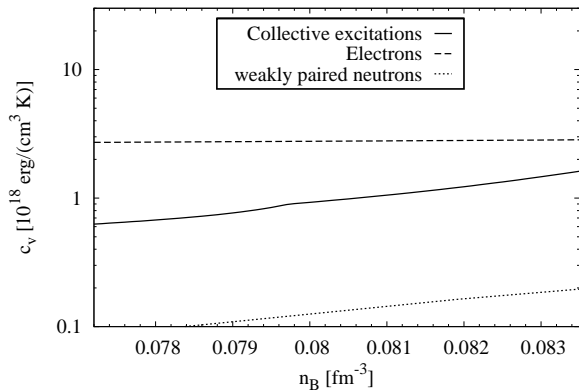


FIG. 3: Different contributions to the specific heat in the density range where one expects to find the lasagna phase, for $T = 10^9$ K. Solid: collective modes, dashed: electrons, dotted: neutron quasiparticles (from Ref. [17]). Concerning the conversion between astrophysical and nuclear units, note that 10^9 K = $86.17k_B^{-1}$ keV and 10^{18} erg K^{-1} cm^{-3} = $7.246 \times 10^{-6}k_B$ fm^{-3} .

generate and its contribution to the specific heat reads

$$c_v^{\text{el.}} = \frac{k_B^2 \mu_e^2 T}{(\hbar c)^3}. \quad (34)$$

The importance of the collective modes becomes clear if one considers the contribution of the gapped neutron quasiparticles (dotted curve), taken from Ref. [17]: In the absence of collective modes, an excitation of the neutron gas requires the breaking of Cooper pairs, which is suppressed by a factor of the order of $e^{-\Delta/k_B T}$. Even in the case of weak pairing, at the present temperature, this contribution is suppressed by approximately one order of magnitude with respect to the contribution of the collective modes.

In Fig. 4, we show the temperature dependence of the specific heat corresponding to the intermediate-density case discussed in Sec. III A (solid line). For comparison, we again display the specific heat due to the electrons (dashed line). Due to its linear temperature dependence, Eq. (34), the electron contribution is always dominant at low temperature, but at higher temperature, the contribution of the collective modes is comparable or even larger than the electron contribution.

At the low temperatures considered here, which are well below the energy of the first optical branch, the contribution of the collective modes to the specific heat is completely dominated by the two linear branches discussed in the preceding subsection. As is well known [50], the specific heat due to an acoustic branch with a linear dispersion relation, Eq. (27), reads

$$c_v = \frac{2\pi^2 k_B^4 T^3}{15\hbar^3 u_s^3} \equiv bT^3. \quad (35)$$

In the present case, however, we have seen that there is in addition a “two-dimensional” branch which propagates

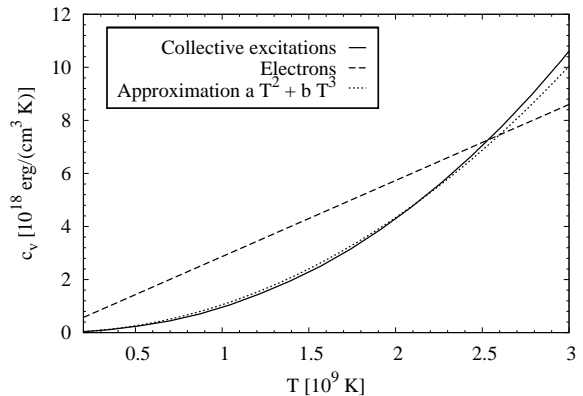


FIG. 4: Temperature dependence of the contribution of the collective modes (solid line) and of the electrons (dashes) to the specific heat for the the example studied in the preceding subsection (see Table I). The approximate formula , $aT^2 + bT^3$, see Eqs. (35) and (36), is shown as a dotted line.

only parallel to the slabs and whose dispersion relation is approximately given by Eq. (31). The contribution of such a mode to the specific heat is readily shown to be

$$c_v = \frac{3\zeta(3)k_B^3 T^2}{\pi\hbar^2 u_s'^2 L} \equiv aT^2, \quad (36)$$

where ζ is the Riemann zeta function [$\zeta(3) = 1.202\dots$]. Due to its quadratic temperature dependence, this is the next dominant contribution at low temperatures after the electrons. The result of the simple formula $aT^2 + bT^3$, where a and b have been calculated with the average values $u_s = 0.078c$ and $u_s' = 0.042c$, is shown as the dotted line in Fig. 4. Up to the temperatures considered here, it fits reasonably well the full calculation.

IV. SUMMARY

In this paper, we have presented a formalism of superfluid hydrodynamics to treat density-wave propagation in inhomogeneous pasta-like nuclear structures which appear in the inner crust of neutron stars. To account for the periodicity of the structure, we incorporate the Floquet-Bloch boundary conditions. The idea is somewhere in between the approaches of Refs. [19, 20], considering only the long-wavelength limit, averaging over the microscopic details of the structure, and microscopic calculations of the crust within the Wigner-Seitz approximation [29, 30], valid for wavelengths smaller than the radius of the Wigner-Seitz cell. Concerning the microscopic input for the nuclear equation of state and the geometry of the structure, we followed the work by Avancini et al. [10].

Within this approach, we have calculated the excitation spectrum of a periodic structure of parallel slabs, the lasagna phase. We have shown that the structure

can indeed induce non-negligible effects on the excitation spectrum. In particular, we found that the sound velocity of the usual acoustic mode depends on the direction of the propagation, and, more surprisingly, that there is a second acoustic mode whose dispersion relation is almost independent of q_z . In addition, we found different optical branches, similar to the phonon spectrum of ordinary crystals.

We have calculated the specific heat corresponding to this excitation spectrum and found that its contribution is much more important than that of individual neutrons, which is strongly suppressed due to the superfluid gap Δ . At temperatures relevant for neutron stars, the main contributions to the specific heat come from the electrons and from the acoustic collective modes. The latter cannot be obtained within the Wigner-Seitz approximation. Due to the curious sound mode whose energy is independent of q_z , the specific heat due to the collective modes goes like T^2 instead of T^3 . [With the same arguments, one would predict that in a rod structure (spaghetti phase), the specific heat should be linear in T .] However, it is not clear whether this feature survives when the Coulomb interaction, which has been neglected here, will be taken into account.

Of course, in order to treat the complex geometry, we were obliged to make a couple of approximations. Contrary to the microscopic approaches based on the Quasiparticle-Random-Phase-Approximation (QRPA) [29, 30], we rely on the assumption that the modes can be described hydrodynamically, which implies in particular that the local neutron and proton Fermi surfaces stay spherical at all times. This assumption is justified if all spatial variations are slow compared to the superfluid coherence length and the temporal variations are slow compared to the superfluid gap.

Both assumptions are not very well fulfilled. However, we have cited examples where hydrodynamics gives reasonable answers even beyond these very restrictive limits, and we believe that the results are at least qualitatively correct. The most serious limitation of the present work is probably that the Coulomb interaction has been neglected. The Coulomb interaction between the protons results in an additional coupling between neighboring cells, which can have important consequences for the excitation spectrum. In the approaches of Refs. [19, 20], it was accounted for by including the elasticity of the Coulomb lattice. In our more microscopic approach, the Coulomb potential would have to be included from the beginning into the proton chemical potential $\mu_p(\mathbf{r}, t)$ in the Euler equation (2). This is a difficult task which will be left for future studies.

It has to be stressed that the contribution of the collective modes studied here is potentially more important than other contributions, notably the contribution from individual neutrons. Therefore it is interesting to pursue their investigation and to include the additional contribution to the specific heat in studies of neutron star thermal evolution.

Acknowledgments

We are indebted to C. Da Providencia for providing us with the data for densities and geometries of the different pasta phases in the model of Ref. [10] as well as to M. Fortin for providing us with the data of Ref. [17]. We thank S. Chiacchiera, D. Peña, and M. Fortin for discussions. This work was supported by ANR (project NEXEN), and by CompStar, a research networking programme of the European Science Foundation.

-
- [1] D. G. Yakovlev, O. Y. Gnedin, A. D. Kaminker, and A. Y. Potekhin, AIP Conf. Proc. **983**, 379 (2008).
 - [2] P. S. Shternin, D. G. Yakovlev, P. Haensel, and A. Y. Potekhin, Mon. Not. R. Astron. Soc. **382**, L43 (2007).
 - [3] E. F. Brown and A. Cumming, Astrophys. J. **698**, 1020 (2009).
 - [4] O. Y. Gnedin, D. G. Yakovlev, and A. Y. Potekhin, Mon. Not. R. Astron. Soc. **324**, 725 (2001), arXiv:astro-ph/0012306.
 - [5] D. G. Ravenhall, C. J. Pethick, and J. R. Wilson, Phys. Rev. Lett. **50**, 2066 (1983).
 - [6] M. Hashimoto, H. Seki, and M. Yamada, Prog. Theor. Phys. **71**, 320 (1984).
 - [7] K. Oyamatsu, Nucl. Phys. A **561**, 431 (1993).
 - [8] C. J. Pethick and D. G. Ravenhall, Ann. Rev. Nucl. Part. Sci. **45**, 429 (1995).
 - [9] G. Watanabe, K. Sato, K. Yasuoka, and T. Ebisuzaki, Phys. Rev. C **68**, 035806 (2003).
 - [10] S. S. Avancini, L. Brito, J. R. Marinelli, D. P. Menezes, M. M. W. de Moraes, C. Providência, and A. M. Santos, Phys. Rev. C **79**, 035804 (2009).
 - [11] G. Watanabe, K. Iida, and K. Sato, Nucl. Phys. A **676**, 455 (2000), arXiv:astro-ph/0001273.
 - [12] S. S. Avancini, S. Chiacchiera, D. P. Menezes, and C. Providencia, Phys. Rev. C **82**, 055807 (2010).
 - [13] G. Baym, C. Pethick, and D. Pines, Nature **224**, 673 (1969).
 - [14] U. Lombardo and H. J. Schulze, Lect. Notes Phys. **578**, 30 (2001), arXiv:astro-ph/0012209.
 - [15] A. Gezerlis and J. Carlson, Phys. Rev. C **81**, 025803 (2010), arXiv:0911.3907.
 - [16] N. Chamel and P. Haensel, Living Reviews in Relativity **11**, 10 (2008), arXiv:0812.3955.
 - [17] M. Fortin, F. Grill, J. Margueron, D. Page, and N. Sandulescu, Phys. Rev. C **82**, 065804 (2010).
 - [18] D. N. Aguilera, V. Cirigliano, J. A. Pons, S. Reddy, and R. Sharma, Phys. Rev. Lett. **102**, 091101 (2009).
 - [19] C. J. Pethick, N. Chamel, and S. Reddy, Prog. Theor. Phys. Suppl. **186**, 9 (2010), arXiv:1009.2303.
 - [20] V. Cirigliano, S. Reddy, and R. Sharma (2011), arXiv:1102.5379.
 - [21] R. I. Epstein, Astrophys. J. **333**, 880 (1988).

- [22] B. Carter and D. Langlois, Nucl. Phys. B **531**, 478 (1998), arXiv:gr-qc/9806024.
- [23] N. Andersson and G. L. Comer, Mon. Not. R. Astron. Soc. **328**, 1129 (2001), arXiv:astro-ph/0101193.
- [24] B. Carter, N. Chamel, and P. Haensel, Nucl. Phys. A **759**, 441 (2005), arXiv:astro-ph/0406228.
- [25] M. E. Gusakov and P. Haensel, Nucl. Phys. A **761**, 333 (2005), arXiv:astro-ph/0508104.
- [26] B. Carter and E. Chachoua, Int. J. Mod. Phys. **D15**, 1329 (2006), arXiv:astro-ph/0601658.
- [27] B. Carter and L. Samuelsson, Class. Quant. Grav. **23**, 5367 (2006), arXiv:gr-qc/0605024.
- [28] A. D. Sedrakian, Astrophysics and Space Science **236**, 267 (1996).
- [29] N. Sandulescu, Phys. Rev. C **70**, 025801 (2004).
- [30] E. Khan, N. Sandulescu, and N. V. Giai, Phys. Rev. C **71**, 042801 (2005).
- [31] J. W. Negele and D. Vautherin, Nucl. Phys. **A207**, 298 (1973).
- [32] E. M. Lifshitz and L. P. Pitaewskii, *Statistical Physics, Part 2*, Landau and Lifshitz: Course of theoretical physics, vol. 9 (Pergamon Press, 1980).
- [33] N. Chamel and P. Haensel, Phys. Rev. C **73**, 045802 (2006).
- [34] A. L. Fetter and J. D. Walecka, *Quantum Theory of Many-Particle Systems* (McGraw-Hill, New York, 1971).
- [35] G. Tonini, F. Werner, and Y. Castin, Eur. Phys. J. D **39**, 283 (2006).
- [36] M. Urban and P. Schuck, Phys. Rev. A **73**, 013621 (2006).
- [37] M. Baldo and C. Ducoin, Phys. Rev. C **79**, 035801 (2009).
- [38] M. Baldo and C. Ducoin, Phys. Atom. Nucl. **72**, 1188 (2009), arXiv:0902.2552.
- [39] R. Prix, Phys. Rev. D **69**, 043001 (2004).
- [40] A. F. Andreev and E. P. Bashkin, Sov. Phys. JETP **42**, 164 (1975).
- [41] T. Gaitanos, M. D. Toro, S. Typel, V. Baran, C. Fuchs, V. Greco, and H. H. Wolter, Nucl. Phys. A **732**, 24 (2004).
- [42] S. S. Avancini, L. Brito, D. P. Menezes, and C. Providência, Phys. Rev. C **70**, 015203 (2004).
- [43] M. E. Gusakov, E. M. Kantor, and P. Haensel, Phys. Rev. C **79**, 055806 (2009), arXiv:0904.3467.
- [44] M. Borumand, R. Joynt, and W. Kluźniak, Phys. Rev. C **54**, 2745 (1996).
- [45] I. Tolstoy, *Wave Propagation* (McGraw-Hill Inc., New York, 1973).
- [46] J. P. LaHeurte, G. A. Williams, H. Dandache, and M. Zoaeter, Phys. Rev. B **28**, 6585 (1983).
- [47] H. Steinwedel, J. H. D. Jensen, and P. Jensen, Phys. Rev. **79**, 1019 (1950).
- [48] P. Ring and P. Schuck, *The Nuclear Many-Body Problem* (Springer-Verlag, Berlin, 1980).
- [49] G. Floquet, Annales scientifiques de l'Ecole Normale Supérieure **12**, 47 (1883).
- [50] L. D. Landau and E. M. Lifshitz, *Statistical Physics, Part 1*, Landau and Lifshitz: Course of theoretical physics, vol. 5 (Pergamon Press, 1967).
- [51] On the time scales of the collective oscillations we want to study, weak interaction processes transforming neutrons and protons into each other can be safely neglected.